Cover Page

University: Northwestern University

Grant Number: DE-FG02-00ER45810

Grant Title: Nanoengineering of Complex Materials

Project Period: 04/15/2000 – 08/31/2018

Principal Investigator: Samuel I. Stupp, PhD

This is the FINAL report for the award.

1. What are the major goals of the project?
We are primarily interested in two important biomimetic principles, namely, self-assembly based on supramolecular chemistry and the use of these structures to template in organic phases as observed in biomineralization. The projects proposed are inspired by some of our achievements in the previous funding period described above, and also by preliminary data gathered recently which we describe below. In addition to our broad objective of acquiring knowledge in supramolecular self-assembly and templating of organic–inorganic hybrid materials, we also propose here work on biomolecular structures based on DNA, peptide nucleic acids, and peptides which can serve as models for artificial materials based on biomimetic principles. The proposed work is divided into three sections, supramolecular systems, hybrid systems, and biomolecular and biological systems. In terms of functions, we are using systems that have relevance to solar cells, catalysis, dynamic/active materials, and ferroelectrics.

2. What was accomplished under these goals?

Major Activities: (8000 characters max)

Semiconducting Arrays of Charge Transfer Complexes

Intermolecular charge transfer complexes, between complementary donor and acceptor small molecules, have functionality predicated on the supramolecular assembly of the molecules. During this funding period, we have investigated the assembly-driven electronic properties of complementary naphthalene donor and pyromellitic diimide acceptor molecules, functionalized with urea and sulfonamide hydrogen bonding motifs. Tetraethylene glycol linkers were incorporated onto the chemical structure to impart solubility in organic solvents. The competition between hydrogen bonding and charge transfer interactions between the complementary molecules led to the formation of charge transfer dimers in solution, and phase separated arrays of donor and acceptor supramolecular assemblies once cast into a thin film. Interestingly, residual charge transfer between the phase separated donor and acceptor arrays led to a boost in electrical conductivity and charge carrier mobility in these films. Hydrogen bonding was shown to play a crucial role in defining the long-range order necessary for charge carrier motion between electrodes (Fig. 1).

Supramolecular Charge Transfer Peptide Amphiphiles

We have also investigated supramolecular exchange between peptide amphiphile (PA) assemblies, driven by charge transfer interactions between complementary donor and acceptor moieties. These systems integrate aromatic donor and acceptor moieties, to the hydrophobic core of the PA nanostructures. Specifically, we synthesized two PA molecules, both containing an alternating valine-lysine tetrapeptide amino acid sequence on one end, and a linear alkyl at the other (Fig. 2A). At the hydrophobic segment of the amphiphile, we tethered either a dialkoxynaphthalene electron donor or a naphthalene diimide electron acceptor. Co-assembly of the donor and acceptor molecules under mildly acidic or basic conditions drives the formation of a charge transfer complex. That both donor and acceptor moieties are chromophores allowed them to be used as tags to track bulk supramolecular exchange. Mixing pre-assembled donor PA nanostructures with acceptor PA nanostructures saw near instantaneous mixing. The kinetics of this exchange is likely driven by charge transfer between the complementary donor and acceptor moieties (Fig. 2).

Conductive Hydrogels From 1D Assemblies of Tripodal Bridged Triarylamines

During this funding cycle, we have developed hybrid inks for the extrusion printing of flexible conductive films. The inks are composed of supramolecular fibers assembled from carbonyl-bridged triarylamine (CBT) chromophores and alginate, a naturally occurring polysaccharide (Fig. 3). Alginate is an ideal component for extrusion inks due to its high viscosity which allows for good flow control through the print head and ability to form robust hydrogels immediately upon contact with a calcium chloride coated substrate. At low concentrations (~0.5 wt%), alginate has a viscosity over a magnitude higher than water and forms ionically-crosslinked gels with storage moduli around 1 kPa. This combination allows for shear alignment of the nanostructures along the during extrusion and locks the alignment by rapid gelation upon contact with divalent calcium ions on the substrate surface. Two different CBTs bearing different functional groups were investigated in this work. The assembly of the CBTs was first studied in water to determine if fibers could be formed. It was also important to investigate how the assembly of chromophores alters the electronic properties of the resulting nanostructures as this will determine if the assembles are relevant for flexible electronics. Different ink compositions were tested varying the amount of the supramolecular and covalent polymer components. Matching the ink viscosity and gelation ability is important to make highly aligned gels with improved electrical performance.

Enhanced out-of-plane conductivity in n = 1 layered perovskites

We have also sought to apply our expertise in the area of chromophore self-assembly and hybrid organic-inorganic materials to the field of perovskite solar cells. In this work, we studied *n* = 1 layered perovskites that consist of alternating organic and inorganic layers with the compound formula $(R\text{-}NH_3^+)_2PbI_4$. Materials of this type are stable to environmental conditions but have poor photovoltaic performance due to the typically insulating nature of the $R\text{-}NH_3^+$ cation. Additionally, these materials tend to orient with the conductive inorganic layers parallel to the substrate which necessitates conductivity through these insulating layers. Here we study cations containing naphthalene, pyrene, and perylene with the goal of improving conductivity perpendicular to the inorganic layers through better aligning the HOMO and LUMO of the organic layer to the inorganic layer (Fig. 4). It was found that improved HOMO–LUMO alignment resulted in several orders of magnitude improvement in conductivity as well as an order of magnitude improvement in power conversion efficiency compared to the prototypical $(butyl\text{-}NH_3^+)_2PbI_4$ layered perovskite.

Organic Solar Cells

The goal of this work is to determine the effect of intermolecular interactions on morphology of the active layer of organic solar cells and the corresponding efficiencies. We introduce hydrogen-bonding motifs to small donor molecules that have benzodithiophene (BDT) at the core. A fullerene acceptor was mixed with the donor molecules, to form the active layer of a bulk heterojunction device, whose morphology was characterized by atomic force microscopy (AFM) and X-ray analysis. We used *n*-dodecylmelamine as a hydrogen bond competitor (**C**), in an attempt to tune the strength of the hydrogen bonding among the BDT molecules and hence control the morphology. Molecule **C** can hydrogen bond to the terminal uracil group of BDT-UrH through a 3-fold H-bonding as in Fig. 8, preventing direct hydrogen-bonding between two **BDT-UrH** molecules. Solar cells were fabricated **BDT-UrH**, **BDT-UrMe**, or **BDT-UrH** and the power conversion efficiency (PCE) was measured for each.

Peptide-Oligonucleotide Supramolecular Systems

As part of this DOE grant, we have recently designed dynamic systems of peptides and DNA that take advantage of the highly reversible and programmable nature of DNA. These systems can be used to control the presentation of chemical signals and surface properties of materials. We began by developing the chemistries needed to integrate oligonucleotides into PA nanostructures to create reversible materials that could switch between sol and gel states. We were able to conjugate single-stranded DNA to PA nanostructures using two different synthetic approaches. The first approach involves copper-free click coupling to an azide-containing PA. In a second approach, we synthesized PA-peptide nucleic acid (PA-PNA) conjugates using solid-phase synthesis. PA-DNAs and PA-PNAs can be co-assembled with PA molecules that lack the nucleotides but have the same chemical structure in the PA segment of PA-DNAs and PA-PNAs. This leads to the assembly of a network of nanofibers that display sequences of nucleotides on their surfaces. We pursued the development of supramolecular materials using nanofibers displaying complementary strands that could crosslink through Watson–Crick base pairing. These crosslinks could then be reversed by 'toehold approach', in which a single stranded DNA displaces another strand through competitive binding (see Fig. 9).

Specific Objectives*:* (8000 characters max)

Semiconducting Arrays of Charge Transfer Complexes

The goal of this project was to understand the interplay between hydrogen bonding and intermolecular charge transfer interactions, and the role they play in the assembly and semiconducting properties of supramolecular thin films. Charge transfer complexes offer a wealth of the structure-property relationships, ranging from ferroelectricity is mixed stack motifs to metallic conductivity in segregated stacks. Introducing structure-directing hydrogen bonding interactions offers another handle to tune the supramolecular assembly, and thus the electronic properties, of these charge transfer complexes.

Supramolecular Charge Transfer Peptide Amphiphiles

Intermolecular charge transfer complexation between aromatic donor and acceptor molecules results in the formation of a discrete charge transfer absorption band, one that is only present when the two complementary molecules are in close proximity to each other. Our goal is to utilize charge transfer as a way to track the interactions between two discrete supramolecular PA assemblies, namely by labelling one PA molecule with the electron donor and the other with the electron acceptor. In this way, we can use optical characterization (namely absorption and fluorescence emission) to track the intermolecular interaction and exchange between the two supramolecular assemblies.

Conductive Hydrogels From 1D Assemblies of Tripodal Bridged Triarylamines

The goal of this work was to investigate the differences in assembly and conductivity of CBT fibers with different non-covalent interactions. Two CBTs were synthesized, one containing amide groups (**CBT1**), which can participate in hydrogen bonds within or between assembles, and another containing alkyne linkages (**CBT2**) that offer no specific interactions to drive assembly (Fig. 3). It was also critical to understand how the different CBT fibers interacted with

alginate during the printing and gelation process. The inks need to have appropriate viscosity and gelation kinetics to form function hydrogels via extrusion printing.

Enhanced out-of-plane conductivity in n = 1 layered perovskites

The goal of this work was to determine the influence of chromophores of naphthalene, pyrene, and perylene on the conductivity perpendicular (out-of-plane) to the inorganic layers in $n = 1$ layered perovskite. Our goal was then to leverage this enhanced out-of-plane conductivity to improve the performance of environmentally stable $n = 1$ layered perovskite solar cells (Fig. 4).

Organic Solar Cells

Most organic semiconductors benefit from π-π stacking, where delocalization reduces the bandgap and enhances the charge mobility. In organic solar cells, the mixing of acceptors and donors affects the PCE of the cells. Our previous work has shown that intermolecular hydrogen bonding can frustrate the π-π stacking resulting in better mixing of the donors and acceptors and smaller donor domain sizes. However, according to some literature reports, intermolecular hydrogen bonding can also be detrimental to solar cell efficiency due to low crystallinity of the active layer induced as a result of weakened π-π stacking. The ability to tune the morphology of the active materials in organic solar cells and its influence on solar cell PCE was investigated.

Peptide-Oligonucleotide Supramolecular Systems

Despite recent advances in creating artificial hierarchical systems through self-assembly, approaches to manipulate these structures reversibly across length scales that reach macroscopic dimensions remain elusive. For example, collagen-mimetic peptides have been reported that form in which triple helices of molecules interact to create fibrillar networks, but these structures are neither tunable nor reversible. Synthetic bundled fibrous networks with the dimensional tunability and dynamic reversibility of collagen would greatly enhance our ability to design functional soft matter. In this work, we report on fibrous supramolecular networks that form reversible superstructures controlled externally by the addition of soluble molecules.

Significant Results: (8000 characters max)

Semiconducting Arrays of Charge Transfer Complexes

We designed and synthesized complementary dialkoxynaphthalene donor and pyromellitic diimide acceptor molecules, functionalized with urea and sulfonamide hydrogen-bonding moieties, respectively (Fig. 1A). Upon co-assembly in organic solvents, these molecules formed dimeric charge transfer complexes, as shown by UV-Vis absorption and fluorescence spectroscopy (Fig. 1B,C). Casting these complexes into thin films resulted in phase separation into discrete arrays of donor and acceptor assemblies by AFM (see Fig. 1D) and X-ray scattering. UV-Vis absorption of the films confirmed the presence of residual charge transfer interactions despite phase segregation. We hypothesize that this residual charge transfer is the cause of the increased conductivity (Fig. 1E) and charge carrier mobility observed in the films of charge transfer complexes. The importance of structure-directing hydrogen bonding was also established by the lower conductivity in charge transfer films of control molecules that did not contain complementary ureas and sulfonamides.

Supramolecular Charge Transfer Peptide Amphiphiles

We synthesized tetrapeptide donor and acceptor molecules that self-assemble into ribbon-like supramolecular assemblies under mildly acidic or mildly basic conditions as shown by cryo-TEM (see Fig. 2B,C) and confirmed by AFM and X-ray scattering. Co-assembly of the donor and acceptor molecules under mildly acidic conditions results in quenching of the naphthalene fluorescence emission due to charge transfer between the donor and acceptor moieties (Fig. 2D). Mixing pre-assembled solutions of donor PAs with acceptor PAS led to immediate supramolecular exchange, characterized by quenching of the donor emission fluorescence (Fig. 2E). Mixing the donor assemblies with a control PA assembly that did not contain the acceptor moiety did not result in quenching, confirming that the supramolecular exchange is driven by charge transfer interactions between donor and acceptor molecules. The nearly instantaneous quenching suggests a rate of exchange that is far greater than that previously observed for supramolecular assemblies. Time-resolved fluorescence spectroscopy and molecular dynamics simulations are currently underway to understand the driving forces and conformational changes that govern supramolecular exchange in this system.

Conductive Hydrogels From 1D Assemblies of Tripodal Bridged Triarylamines

We synthesized two novel CBT compounds, **CBT1** with arms attached via an amide and **CBT2** through an alkyne linkage. Both compounds were observed to form fibers in basic water (Fig. 3A,B), but the photophysical properties of the two dyes were quite different. **CBT1** exhibited an almost complete quenching of fluorescence when assembled in water compared to the monomer in DMSO, consistent with face-to-face stacked H-aggregates (Fig. 3C). In contrast, **CBT2** displayed a red shift in its fluorescence in water with reasonably strong intensity signifying the formation of slip-stacked J-aggregates (Fig. 1D). The conductivity of **CBT1** was approximately two orders of magnitude greater than **CBT2** making it a better candidate for flexible conductive films. An ink containing 1.5 wt % **CBT1** and 0.5% alginate was found to be a good ratio for easy printing and stable gel formation. The printed films contained highly aligned fibers and were stable to multiple rounds of bending, while retaining their electrical conductivity. In a transistor geometry, both materials exhibited ambipolar transfer curves with slightly higher hole mobilities than electron mobilities (Fig. 3F). Similar to the conductivity measurements, we observed roughly an order of magnitude higher hole mobility for the **CBT1** films than the **CBT2** films (0.194 vs. 0.0178 cm2/V-s).

Enhanced Out-of-Plane Conductivity in n = 1 Layered Perovskites

We synthesized a total of seven ammonium-iodide salts containing naphthalene, pyrene, or perylene and crystalized these into the corresponding $n = 1$ layered perovskite. The structure was determined by X-ray crystallography. These crystals were then placed on a conductive substrate and gold pads evaporated on top. The conductivity was then measured through the thickness of these crystals (Fig. 5). Conductivity increases with increasing aromatic content from the aliphatic controls to the perylene crystals, as expected from the energy level alignment (Fig. 4). Photovoltaic devices were fabricated from one of the pyrene-containing perovskites. These devices showed a PCE of 1.1 ± 0.1% (Fig. 6), which represents over an order of magnitude improvement over the best previously reported comparable devices.

Organic Solar Cells

We synthesized two symmetric DBT-based small molecules (Fig. 7). The first molecule (**UrH**) contains a uracil hydrogen-bonding moiety. The second molecule (**UrMe**) contains a methylated

uracil group, which does not have any hydrogen bond donors. The optoelectronic properties of the two molecules, using UV-vis and ultra-violet photoelectron spectroscopy, were found to be very similar, as shown in the energy level diagram (see Fig. 8B). Solar cell devices were fabricated with the architecture depicted in Fig. 8A. By analyzing grazing-incidence wide-angle X-ray scattering (GIWAXs) pattern of the active layer of these two molecules, we found that the **UrH** forms amorphous films, whereas the **UrMe** forms more crystalline films with distinct π–π stacking (Fig. 9A). AFM shows significantly larger domains **UrH** for relative to **UrMe** (Fig. 9B). The amorphous **UrH** solar cells yielded low PCE compared to **UrMe** (see I–V curves in Fig. 8C) and the external quantum efficiency (EQE) dramatically decreased for the less crystalline hydrogen-bonding molecule **UrH** (Fig. 8D). However, adding small molecule **C** to the system increased the degree of crystallinity of the **UrH**, which blocks **UrH** from forming hydrogen bonding with the other **UrH** molecules. Upon addition of molecule **C**, increased crystallinity and reduced the domain size improved both the PCE and EQE.

Peptide-Oligonucleotide Supramolecular Systems

We formed gels of the PA-DNA hybrids and we were surprised to find by electron microscopy two apparent phases consisting of large micrometer-sized bundles of fibers enriched with DNA that segregated within a network of DNA-depleted individual fibers (see Fig. 10B). The enrichment of DNA in the bundled regions was established using fluorescently labeled DNA segments. We hypothesized that formation of the bundled regions requires “large scale” dynamic redistribution of monomers within and among the fibers, creating a hierarchical structure which is reversible with temperature or toehold addition. Coarse-grained molecular dynamics simulations, in collaboration with Erik Luijten at Northwestern, suggest that dynamic molecular exchange over large spatial distances among the supramolecular assemblies is necessary to form the DNA-rich bundles. In an effort to understand how the observed bundled superstructures form, we mixed dilute solutions of assemblies with complementary strands of DNA, in which all molecules of the assembly contained the nucleic acid segment. These assemblies formed spherical micelles in their respective solutions, but transformed upon mixing into intertwined nanoscale filaments that grew into larger bundles over the course of seven days (see Fig. 10C,D). Interestingly, a coarse-grained simulation of the interacting filaments with complementary DNA segments recreated the intertwined fibers and the observed pitch observed by electron microscopy (300 nm) (see Fig. 10c). We hypothesize that these structures are non-equilibrium kinetic structures that bend around each other rather than interact parallel to each other to produce the maximum hybridization by Watson–Crick pairing. Their intertwining leaves free non-hybridized DNA on their surfaces so they can continue to grow into superstructures.

Key Outcomes or Other Achievements (8000 characters max)

Semiconducting Arrays of Charge Transfer Complexes
These findings will be submitted for publication soon.

Narayanan, A.; Barreda, L.; Sai, H.; Passarelli, J. V.; Dannenhoffer, A. J.; Aytun, T.; Fairfield, D. J.; Moy, E. C.; Palmer, L. C.; Stupp, S.I. “Co-Assembly and Phase Separation in Semiconducting Hydrogen-Bonded Charge Transfer Complexes” *Manuscript in Preparation*.

Supramolecular Charge Transfer Peptide Amphiphiles

These findings will be submitted for publication, once the proposed experiments and simulations to confirm modulate the driving forces for exchange are complete.

Conductive Hydrogels From 1D Assemblies of Tripodal Bridged Triarylamines
These findings will be submitted for publication soon.

Sather, N. A.; Dannenhoffer, A. J.; Zambrotta, R. F.; Sangji, M. H.; Stupp, S. I. “Biopolymer-Supramolecular Polymer Hybrids as Anisotropic Soft Semiconductors” *Manuscript in Preparation*.

Enhanced out-of-plane conductivity in n = 1 layered perovskites

These results were recently published.

Passarelli, J. V.; Fairfield, D. J.; Sather, N. A.; Hendricks, M. P.; Sai, H.; Stern, C. L.; Stupp, S. I. "Enhanced Out-of-Plane Conductivity and Photovoltaic Performance in *n* = 1 Layered Perovskites Through Organic Cation Design" *J. Am. Chem. Soc*. **2018**, *140*, 7313-7323.

Organic Solar Cells

These findings will be submitted for publication soon.

Leonel Barreda, Jiahao Chen, James Passarelli, Adam Dannenhoffer, Daniel D. Fairfield, and Samuel I. Stupp “Intermolecular Hydrogen Bonding in Small-Molecule Organic Solar Cells” *Manuscript in preparation.*

Peptide-Oligonucleotide Supramolecular Systems

These results were published recently.

Freeman, R.; Han, M.; Álvarez, Z.; Lewis, J. A.; Wester, J. R.; Stephanopoulos, N.; McClendon, M. T.; Lynsky, C.; Godbe, J. M.; Sangji, H.; Luijten E.; Stupp, S. I. "Reversible Self-Assembly of Superstructured Networks" *Science In Press.* (2018) DOI: 10.1126/science.aat6141

3. What opportunities for training and professional development has the project provided?

During the funding period, this project has directly provided training opportunities for five graduate students and three post-docs. These students have received direct technical training through their cross-disciplinary laboratory research experience as well as mentoring from the P.I. and from senior group members. The project has also given the opportunity to host five undergraduate students to conduct research in the group and gain hands-on research experience.

4. How have the results been disseminated to communities of interest?

[If there is nothing significant to report during this reporting period, state “Nothing to Report.” Describe how the results have been disseminated to communities of interest. Include any outreach activities that have been undertaken to reach members of communities who are not usually aware of these research activities, for the purpose of enhancing public understanding and increasing interest in learning and careers in science, technology, and the humanities.]

Nothing to report

Products

Sato, K., Hendricks, M. P., Palmer, L. C. & Stupp, S. I. Peptide supramolecular materials for therapeutics. Chem. Soc. Rev. 47, 7539–7551 (2018).

Passarelli, J. V. et al. Enhanced Out-of-Plane Conductivity and Photovoltaic Performance in *n* = Layered Perovskites through Organic Cation Design. J. Am. Chem. Soc. 140, 7313–7323 (2018).

Lau, G. C. et al. Oriented Multiwalled Organic-Co(OH)2 Nanotubes for Energy Storage. Adv. Funct. Mater. 28, (2018).

Hendricks, M. P., Sato, K., Palmer, L. C. & Stupp, S. I. Supramolecular Assembly of Peptide Amphiphiles. Acc. Chem. Res. 50, 2440–2448 (2017).

Rubert Pérez, C. M., Álvarez, Z., Chen, F., Aytun, T. & Stupp, S. I. Mimicking the Bioactivity of Fibroblast Growth Factor-2 Using Supramolecular Nanoribbons. ACS Biomater. Sci. Eng. 3, 2166–2175 (2017).

Lee, S. S. et al. Sulfated glycopeptide nanostructures for multipotent protein activation. Nat. Nanotechnol 12, 821–829 (2017).

Narayanan, A. et al. Ferroelectric Polarization and Second Harmonic Generation in Supramolecular Cocrystals with Two Axes of Charge-Transfer. J. Am. Chem. Soc. 139, 9186–9191 (2017).

Ortony, J. H. et al. Water Dynamics from the Surface to the Interior of a Supramolecular Nanostructure. J. Am. Chem. Soc. 139, 8915–8921 (2017).

Kazantsev, R. V. et al. Crystal-Phase Transitions and Photocatalysis in Supramolecular Scaffolds. J. Am. Chem. Soc. 139, 6120–6127 (2017).

Deiss-Yehiely, E., Ortony, J. H., Qiao, B., Stupp, S. I. & Olvera de la Cruz, M. Ion condensation onto self-assembled nanofibers. J. Polym. Sci. Pol. Phys. 55, 901–906 (2017).

IMPACT

1. What is the impact on the development of the principal discipline(s) of the project?

Our recent accomplishments have far reaching impact in the design of functional self-assembled structures. In particular, we have developed materials based on materials with a high degree of internal order, such as hierarchically organized membranes and phase separated peptide nanofibers with DNA.
Understanding how to control the formation of these kinds of materials presents broader opportunities to design new, highly ordered materials with functions like photovoltaics, energy storage or photocatalysis. The hybrid covalent–noncovalent polymer system has great potential to inspire new directions in dynamic, responsive, and recyclable materials.

2. What is the impact on other disciplines?

Outside the field of energy-related materials, the fundamental self-assembly behavior and dynamics of the DNA–peptide hybrids have inspired new work in biomaterials that is supported by other grants. This work is specifically directed at controlling cellular behavior using molecular signals that can be presented to cells or suppressed in a reversible manner. In particular, the dynamic supramolecular systems enabled us to discover how changes in architectural features in fibrous hydrogel networks can modulate important phenotypic transformations in astrocytes linked to brain and spinal cord injury as well as neurological diseases.

3. What is the impact on the development of human resources?

This project has opened up a number of valuable teaching and mentoring opportunities within our research group. This grant supports students and postdocs in their development as scientific researchers. They have had the opportunity to develop technical research skills by conducting research in a highly interdisciplinary group with access to diverse, world-class experimental facilities and collaborators. They also have the chance to build their oral and written communication skills and develop a career plan through regular interactions with their peers and with their advisor.

4. What is the impact on physical, institutional, and information resources that form infrastructure?

Nothing to report

5. What is the impact on technology transfer?

Nothing to report

6. What is the impact on society beyond science and technology?

Nothing to report.

7. Foreign Spending

Not Provided

17

Tracking #: RPT-0000000928 **PROGRESS REPORT**

CHANGES - PROBLEMS

1. Changes in approach and reasons for change

Nothing to report.
2. Actual or anticipated problems or delays and actions or plans to resolve them
Nothing to report.
3. Changes that have a significant impact on expenditures
Nothing to report.
4. Significant changes in use or care of human subjects, vertebrate animals, and/or biohazards
Nothing to report.
5. Change of primary performance site location from that originally proposed
Nothing to report.
6. Carryover Amount
Estimated carryover amount for the next budget period: $0.00

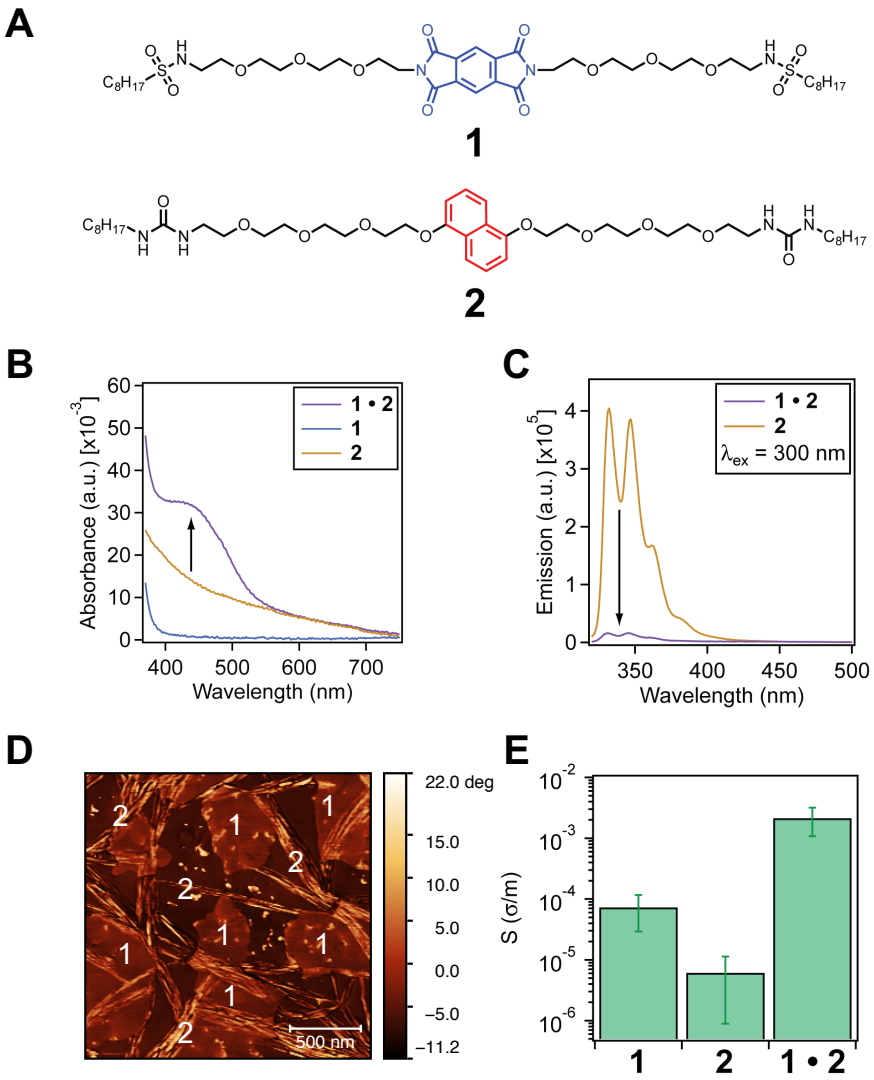

Figure 1: A) Molecular design for pyromellitic diimide-based electron acceptor (**1**) and naphthalene-based electron donor (**2**). Co-assembly of 1 and 2 in toluene results in B) a broad charge transfer absorption band and C) quenching of the naphthalene fluorescence emission. Casting the co-assembled **1●2** into a thin film results in D) phase separation into platelet (acceptor) and fibrous (donor) supramolecular assemblies. Despite phase separation, residual charge transfer interactions drives E) higher thin film conductivity in the co-assembled **1●2** compared to that of the acceptor **1** or the donor **2**.

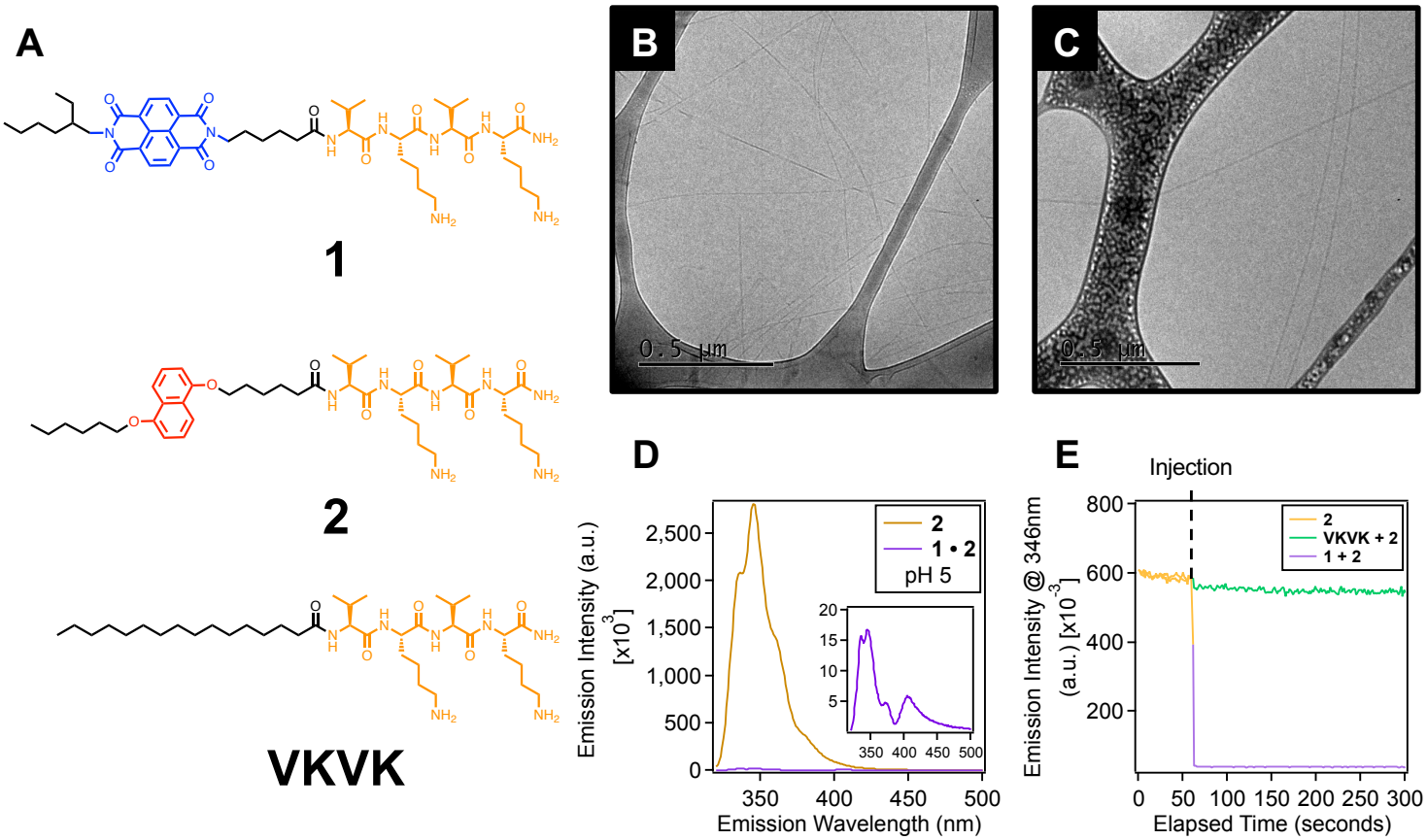

Figure 2: A) Molecular design for peptide amphiphiles incorporating a naphthalene diimide electron acceptor (**1**), dialkoxynaphthalene electron donor (**2**) or linear palmitic acid (**VKVK**). Cryogenic TEM of B) acceptor **1** and C) donor **2** at pH 5 illustrates long-range supramolecular assembly. D) Co-assembly of **1** and **2** results in quenching of the naphthalene fluorescence emission. E) Injecting equimolar quantities of pre-assembled **1** to a solution of pre-assembled **2** results in significant fluorescence quenching due to charge transfer, compared to injecting equimolar quantities of the control **VKVK**. This implies supramolecular exchange between the complementary donor and acceptor assemblies, driven by charge transfer interactions, in a matter of seconds.

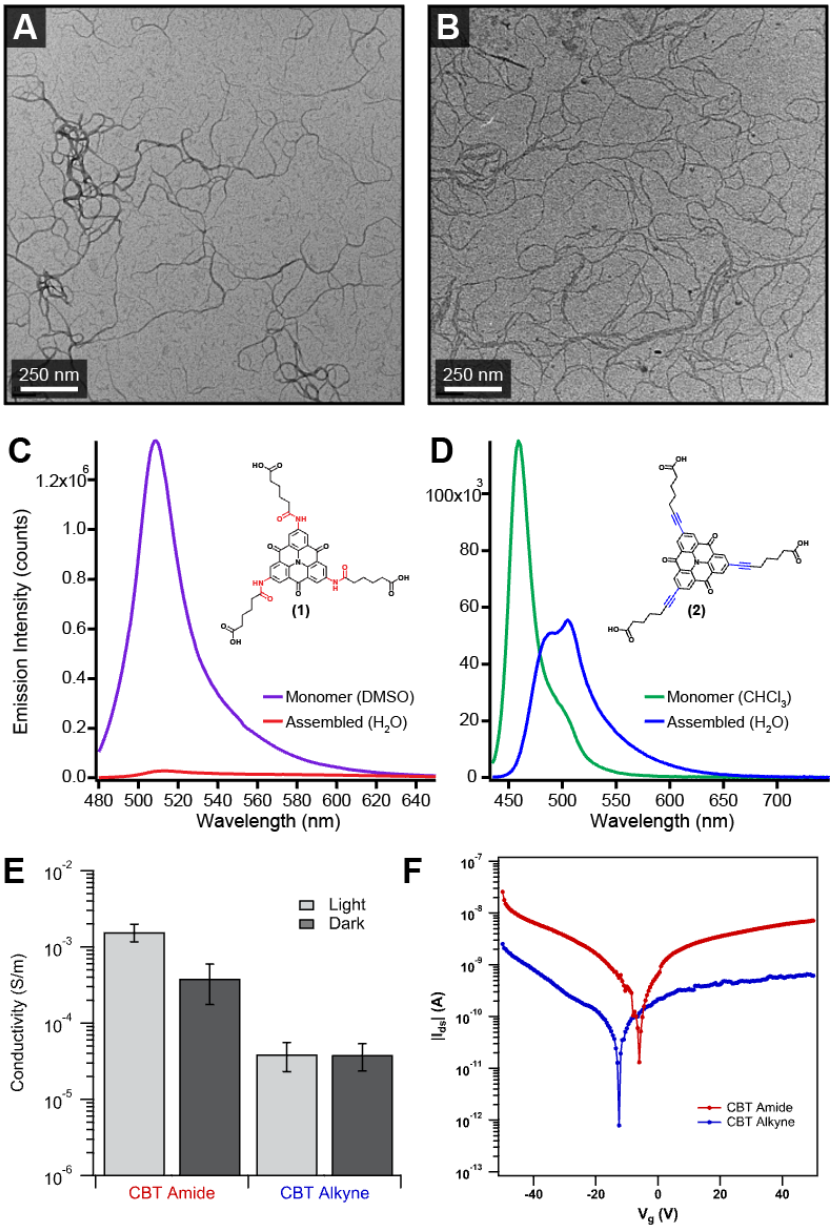

Figure 3: A) TEM of **CBT1**. B) TEM of **CBT2.** C) Fluorescence emission spectra of **CBT1** (10 μm) showing strong quenching due to formation of supramolecular assemblies (λ_{ext} 440 mM). Molecular structure of **CBT1**. D) Fluorescence emission spectra of **CBT2** (10 μm) showing bathochromic shift in emission due to formation of supramolecular assemblies (λ_{ext} 410 mM). Molecular structure of **CBT2**. E) Conductivity of CBT1 and CBT2 from after spin coating. F) Thin-film transistor transfer curves of **CBT1** and **CBT2** films.

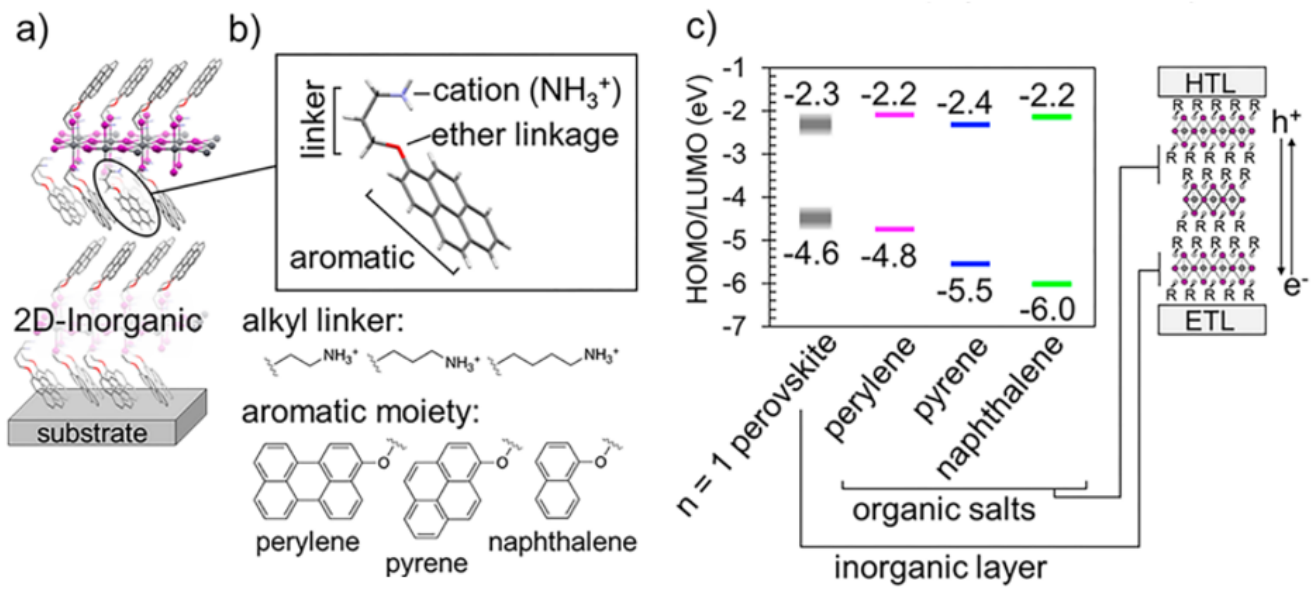

Figure 4. (a) *n* = 1 layered perovskites of the form $(R{-}NH_3)_2PbI_4$ showing alternating organic and inorganic layers that align parallel to the substrate. (b) Modular molecular design of the ammonium iodide cation consisting of an aromatic core joined by an ether bond to an alkyl linker of variable length. (c) Energy levels of typical *n* = 1 layered perovskites (gray) with values specific to $(butyl\text{-}NH_3)_2PbI_4$ as compared to the energy levels of the conjugated organic ammonium iodide salts of interest: perylene-*O*-ethyl-NH_3I, pyrene-*O*-propylNH_3I, and naphthalene-*O*-propyl-NH_3I. HTL and ETL refer to hole and electron transport layers, respectively.

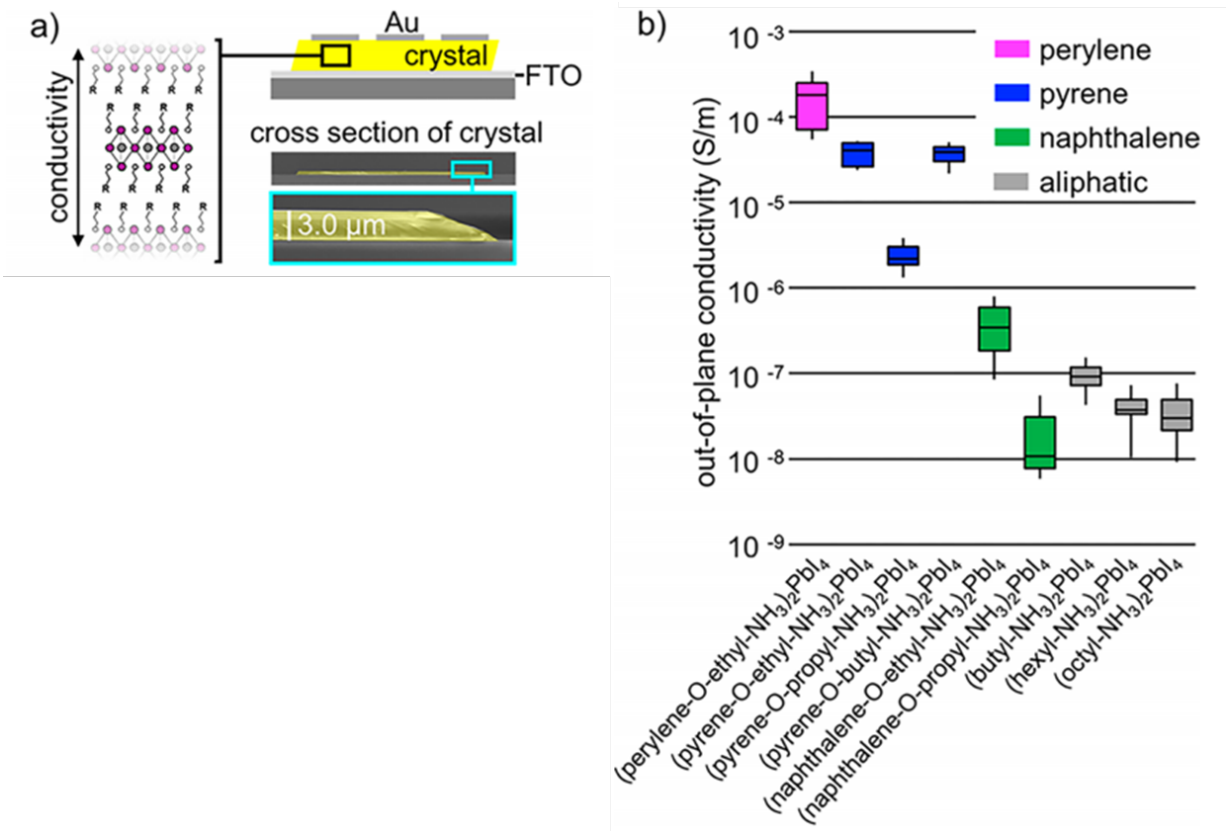

Figure 5. (a) Schematic representation of the layered perovskite indicating the direction of conductivity measurements (left), and schematic of the device used to measure the out-of-plane conductivity and a colorized SEM of a single crystal drop-cast on a silicon wafer cleaved to reveal the cross section (right) (note the crystal is flat over its width (0.5 mm) and makes good contact with the substrate). (b) Conductivity of nine different n = 1 layered perovskites with either an aliphatic cation or a cation containing naphthalene, pyrene, or perylene (higher conductivity is observed for the pyrene and perylene samples, which possess better energy level alignment with the inorganic lattice). FTO refers to fluorine-doped tin oxide.

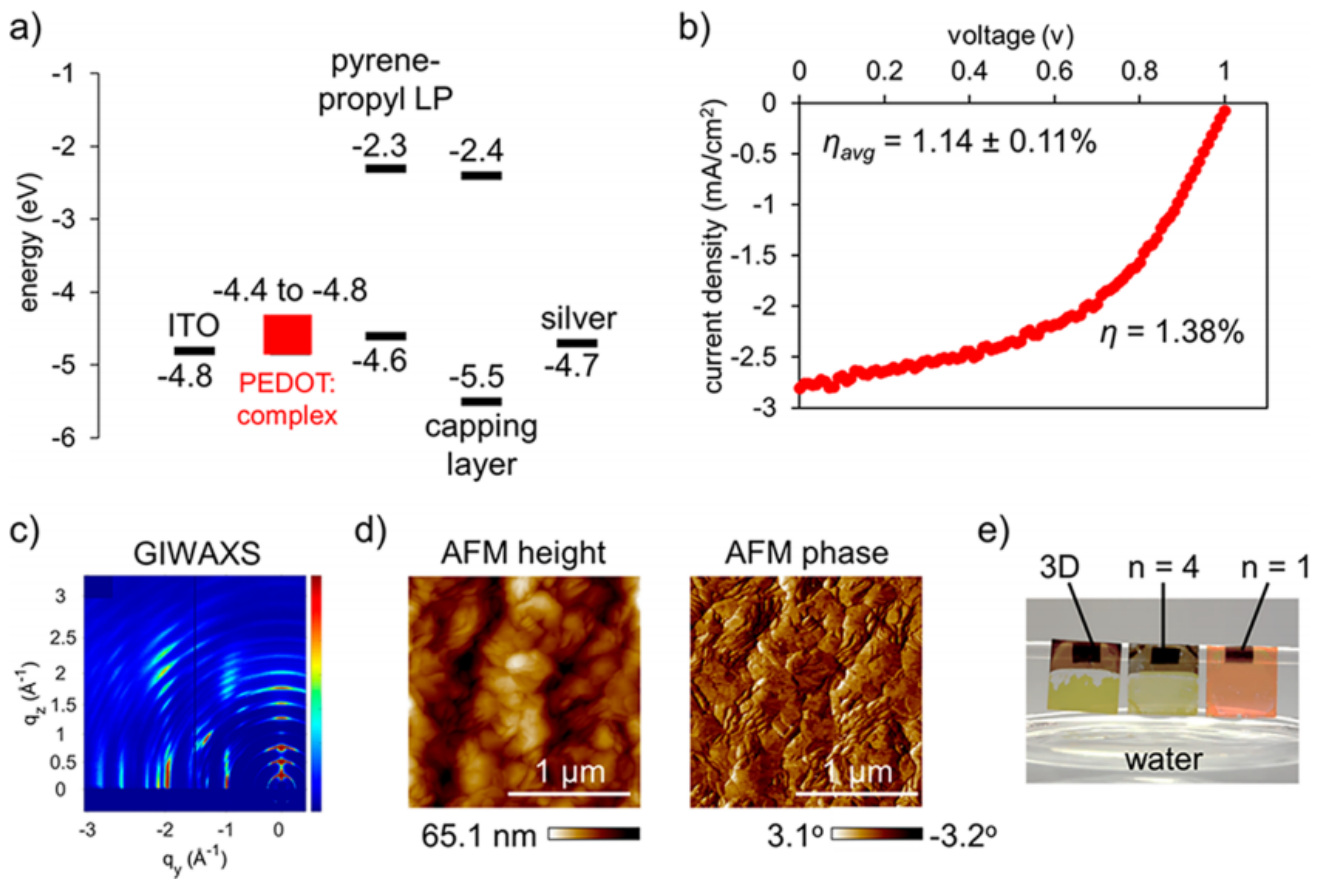

Figure 6. (a) Energy levels of the layers in the (pyrene-*O*-propyl-NH_3)$_2$$PbI_4$ layered perovskite solar cell. (b) I−V curve for the champion device with 1.38% efficiency (only forward sweep is shown for clarity, but the average includes forward and reverse curves where little hysteresis was observed). (c) Grazing-incidence wide-angle X-ray scattering of (pyrene-*O*-propyl-NH_3)$_2$$PbI_4$ crystallized on a PEDOT:PSS-coated substrate. (d) AFM height and phase images for (pyrene-*O*-propyl-NH_3)$_2$$PbI_4$ crystallized on PEDOT:PSS. (e) Photograph showing the appearance of the three substrates dipped in water. The 3D perovskite with the formula (CH_3NH_3)PbI_3 and the n = 4 layered perovskite with the formula (butyl-NH_3)$_2$(CH_3NH_3)$_3$$Pb_4I_3$ turn yellow instantly revealing chemical degradation, whereas the n = 1 layered perovskite (pyrene-*O*-propyl-NH_3)$_2$$PbI_4$ retains its original color.

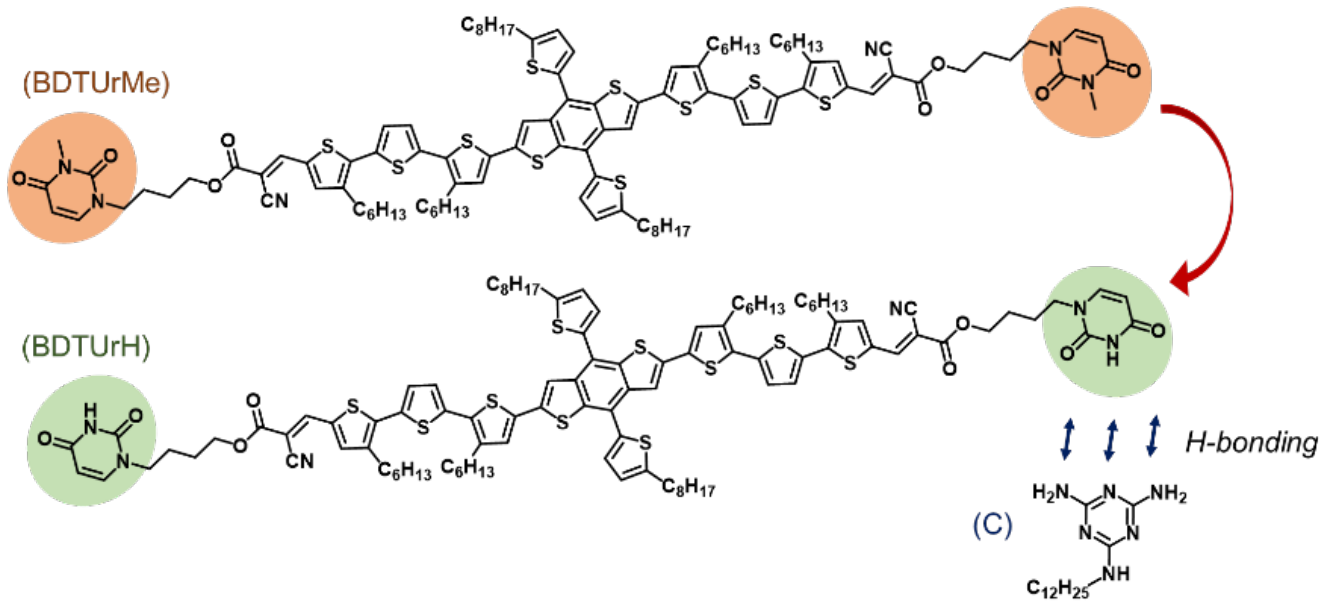

Figure 7. The structure of the molecules that have different terminal groups are used for solar cells.

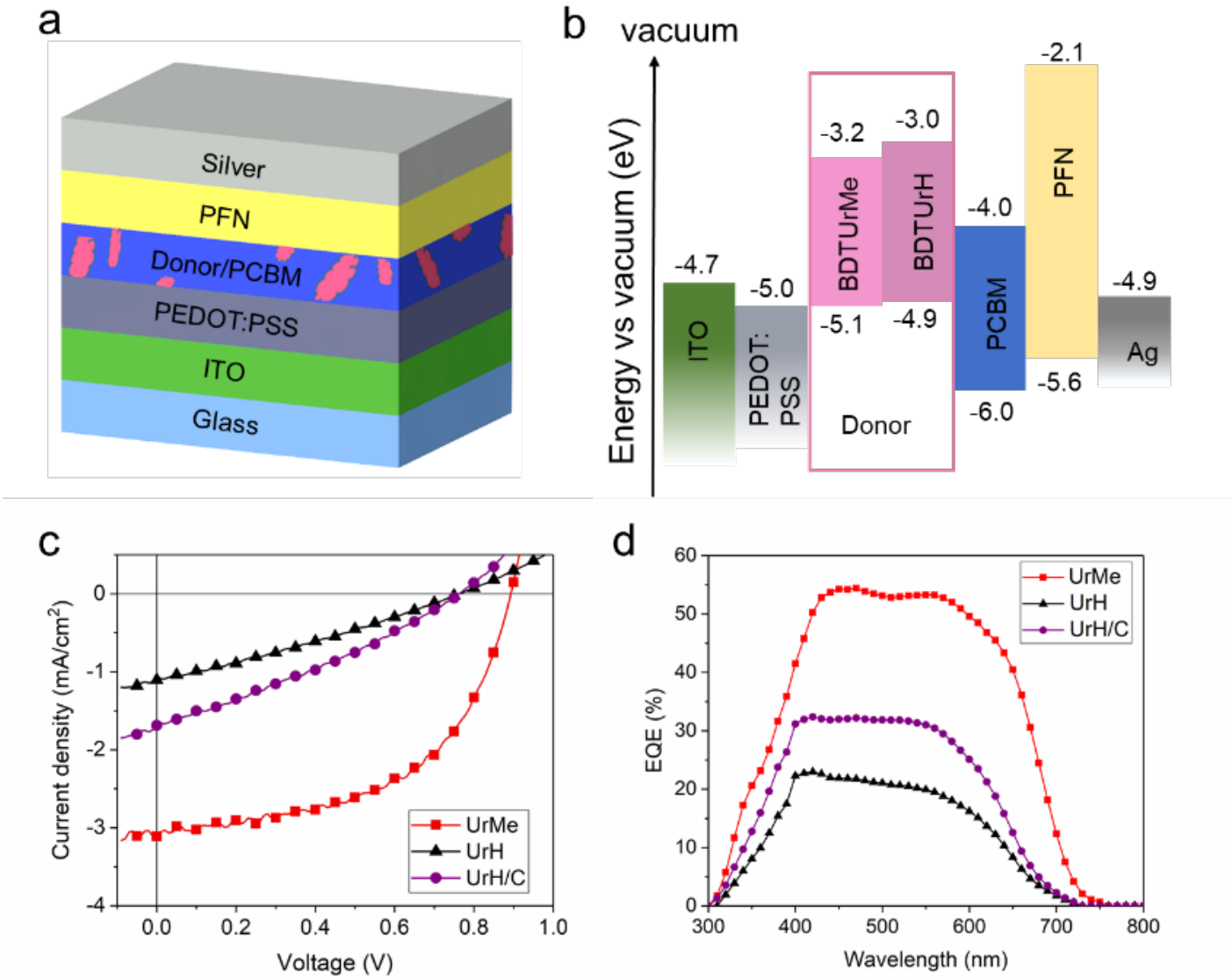

Figure 8. The solar cell device fabrication and testing. A) Schematic of the solar cell device architecture. B) Energy diagram of the layers in the solar cell devices. C) Illuminated I–V curves of the solar cells. D) External quantum efficiency measurement of the solar cells.

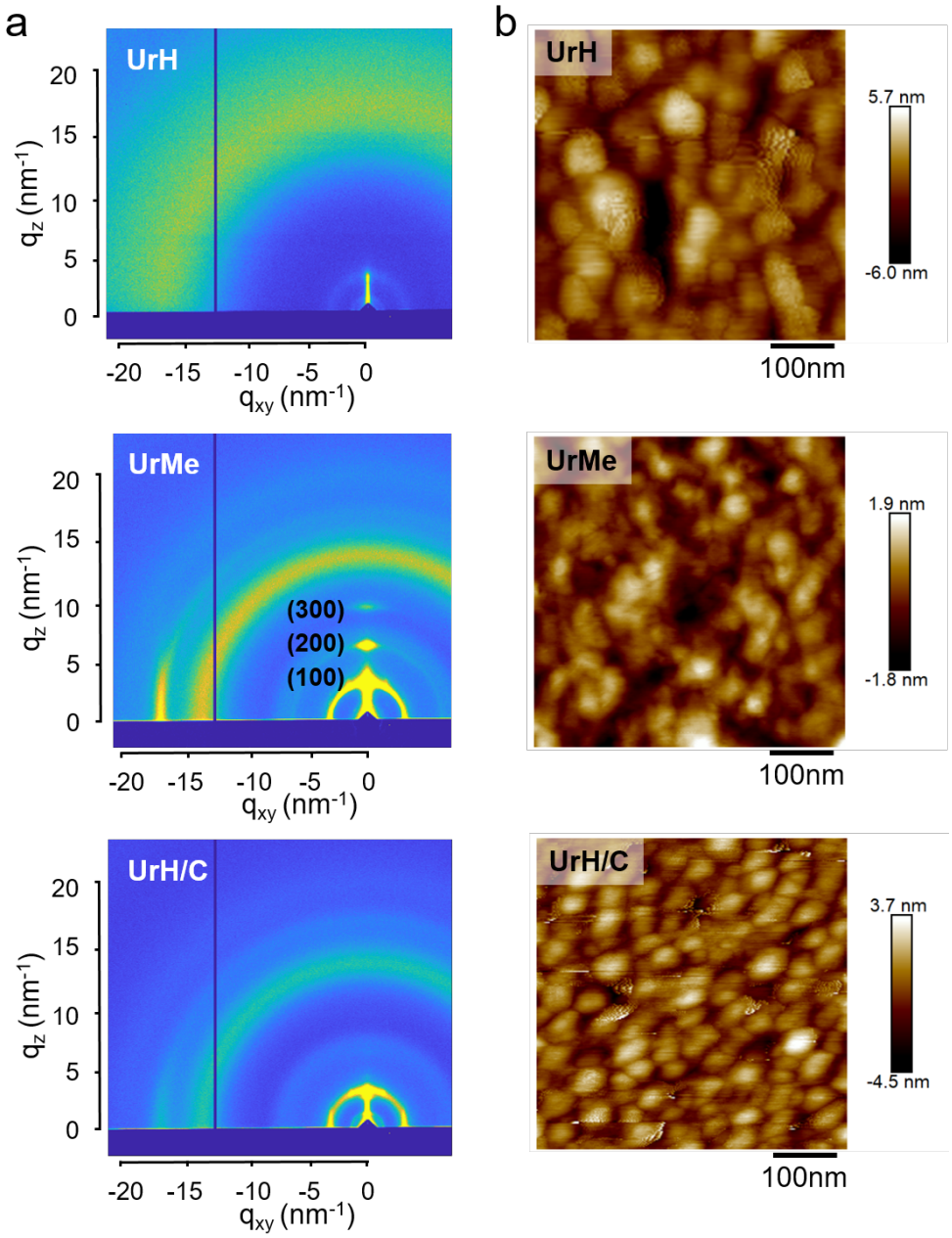

Figure 9: The morphology of the donor/acceptor heterojunction layer. a) The grazing-incidence wide-angle X-ray scattering (GIWAXs) patterns show different crystalline nature of the thin film. b) AFM height images indicate different domain size for those molecules (or with competitor molecule **C**).

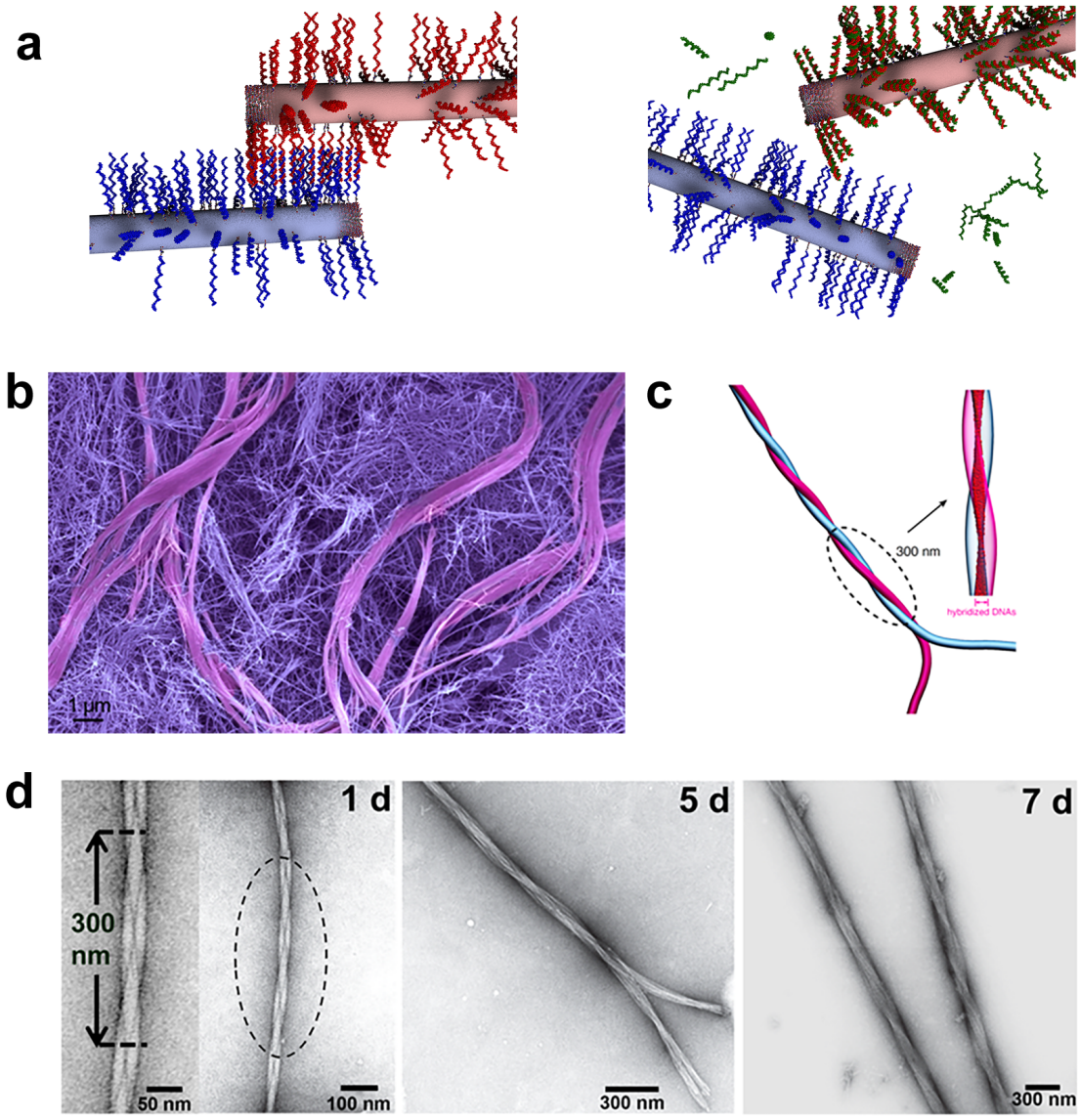

Figure 9. DNA cross-linked PA gels. (a) Mixing two PAs with complementary DNA results in a gel due to the DNA hybridization. Subsequent disruption of the cross-link by strand displacement or with a DNase enzyme results in dissolution of the gel. (b) Scanning electron micrographs of the cross-linked DNA-PA gels. (c) Simulation snapshot of two intertwined complementary fibers. Hybridized DNA-PNA pairs between the two fibers (magnified view) form a twisted ribbon pattern. (d) TEM images after mixing complementary DNA- and PNA-terminated peptide amphiphiles show the time-dependent evolution of twisted bundles after one, five, and seven days.